Molecular-Scale Remnants of the Liquid-Gas Transition in Supercritical Polar Fluids

V. P. Sokhan,[1] A. Jones,[2] F. S. Cipcigan,[1,2] J. Crain,[1,2] and G. J. Martyna[3]
[1]National Physical Laboratory, Hampton Road, Teddington, Middlesex TW11 0LW, United Kingdom
[2]School of Physics and Astronomy, The University of Edinburgh, Mayfield Road, Edinburgh EH9 3JZ, United Kingdom
[3]IBM T. J. Watson Research Center, Yorktown Heights, New York 10598, USA
(Received 14 June 2015; published 11 September 2015)

An electronically coarse-grained model for water reveals a persistent vestige of the liquid-gas transition deep into the supercritical region. A crossover in the density dependence of the molecular dipole arises from the onset of nonpercolating hydrogen bonds. The crossover points coincide with the Widom line in the scaling region but extend farther, tracking the heat capacity maxima, offering evidence for liquidlike and gaslike state points in a "one-phase" fluid. The effect is present even in dipole-limit models, suggesting that it is common for all molecular liquids exhibiting dipole enhancement in the liquid phase.

DOI: 10.1103/PhysRevLett.115.117801 PACS numbers: 61.20.Ja, 31.15.-p, 64.60.F-, 65.20.Jk

There is a distinct boundary between liquid and vapor phases of a substance separated by a coexistence line over a finite range of pressures (p) and temperatures (T). Crossing the line results in a discontinuous density change—the hallmark of a first-order phase transition. The coexistence line terminates at a critical point in the (T, p) plane beyond which the thermodynamic distinction between liquid and gas phases is lost and a single-phase supercritical fluid is formed. In this region, there are no further phase boundaries and the supercritical fluid permits a continuous path from liquid to gas over a broad range of thermodynamic states [1]. In water, for example, this tunability can be exploited to control solvation properties making supercritical water an important ingredient in industrial processes and a promising "green" alternative to chemical solvents [2–4].

While the classical thermodynamic picture is well understood, the molecular nature of supercritical fluids remains a largely open question. Key issues for hydrogen-bonded fluids are (1) structure and hydrogen bonding (HB) in the supercritical region, (2) the electronic redistribution which occurs in the molecules as the HB network is reconfigured, and (3) most broadly, the relationship of the supercritical fluid to fundamental liquid and gaseous states of matter that exist as separate phases below T_c.

In this context, the observation that certain thermophysical response functions exhibit maxima in the transition region between gaslike and liquidlike states of the supercritical phase has prompted the suggestion that a remnant of coexistence may extend into the supercritical region [5]. The locus of such maxima is referred to as the Widom line [6]. Direct confirmation of distinct gaslike and liquidlike state points, however, is lacking though some evidence of dynamical crossover phenomena has been reported in noble gases [5,7]. Analogous concepts may apply at low temperatures where a Widom line is proposed to extend from a hidden liquid-liquid critical point [6] influencing the properties of supercooled water.

Supercritical water, in particular, poses unique challenges for molecular models because conventional empirical interaction potentials capture neither the electronic redistribution which occurs along an isotherm within the supercritical region of the phase diagram (dipole, quadrupole, and higher many-body polarization responses) nor the many-body dispersion forces which have emerged as an important aspect of water physics [8,9]. Moreover, as these empirical models are typically optimized to describe liquid water near ambient conditions, their transferability to the supercritical fluid is questionable and the resulting physical insight into the molecular processes that occur above the critical point is limited.

A new approach for materials simulation has been proposed recently wherein the molecular electronic distribution is not represented by a parametrized mean-field model, but rather by a coarse-grained description based on embedded harmonic oscillators—the quantum Drude oscillator (QDO) model [10,11]. As the oscillators are treated quantum mechanically, this model generates the complete hierarchy of many-body polarization and dispersion phenomena, which when solved in strong coupling, as here, ensures that all potential symmetry-breaking interactions are present within Gaussian statistics. The responses (to all orders) include, but are not limited to, inductive responses leading to distortions of the electronic charge distribution and to van der Waals and higher-order dispersion interactions arising from quantum mechanical charge density fluctuations. The model parameters are fit to leading-order responses of the isolated molecule providing a perfect low-density limit [9,12,13]. Here we apply the model to treat water with the short-range repulsion parametrized to high-level *ab initio* calculations of the dimer (see Refs. [9,14] for model details).

In prior work [9], using the methodology described in Refs. [10–13] to simulate our water model, we have determined the location of its critical point as $\{T_c = 649(2)$ K, $\rho_c = 0.317(5)$ g/cm$^3\}$, which is in accord with experiment

$\{T_c = 647.096$ K, $\rho_c = 0.322$ g/cm$^3\}$ [20]. The dielectric properties along coexistence as well as the orthobaric densities of both the gas and liquid branches are well described [9]. We regard the prediction of an accurate critical point as a prerequisite for reliable examination of the supercritical phase. We are aware of no other description able to predict an accurate critical point from the properties of the isolated molecule.

Having established the critical point and the dielectric properties of the water model, we are now in position to examine the molecular properties across several supercritical isotherms and to draw broader conclusions about the molecular nature of supercritical fluids. To set the context for this part of the work, we draw attention to recent studies that have explored the extent to which the notion of liquid-gas coexistence can be extended past the critical point. Typically, this extrapolation is based on identifying the loci of maxima in second-order thermodynamic response functions such as heat capacity (C_p), thermal expansivity (α), or isothermal compressibility (κ_T) along isothermal paths. In atomic systems (noble gases), evidence of dynamic anomalies near the points of maxima in C_p has been reported [7] and interpreted as a signature of liquidlike and gaslike behavior. However, it is clear that the extrema of different thermodynamic functions rapidly diverge from each other above the critical point and only collapse onto a universal Widom line in the asymptotic scaling region near the critical point as described by a scaling theory developed in Ref. [1]. Beyond this region, and farther into the one-phase supercritical field, it is unclear whether any specific thermodynamic observable separates distinct regimes which can be unambiguously associated with liquidlike or gaslike behavior.

We now consider the dipole moment of water as a local reporter of molecular environment. Individual water molecules that are adaptive and responsive to their environment become strongly polarized as a result of the highly directional bonding of the liquidlike state [21]. We explored the supercritical region along several isotherms from 673 to 1083 K and for densities from 2 to 60 mol/l spanning from 10 MPa to 2.4 GPa. The results of our calculations of the molecular dipole at two isotherms in the supercritical region of the phase diagram are shown in Fig. 1. The dipole's density dependence exhibits a change in slope at $\rho =$ 17.1 mol/l at 673 K and 18.9 mol/l at 873 K. The corresponding densities of heat capacity maxima, obtained from the International Association for the Properties of Water and Steam 1995 Standard (IAPWS-95) reference equation of state for water [20], are 17.25 and 18.91 mol/l. The dipole crossover is still detectable at $T = 1083$ K $= 1.7T_c$, above which it disappears in statistical noise. It becomes more pronounced with decreasing temperature, and below T_c it occurs in the two-phase region.

In order to further investigate the crossover in the dipole moment, we analyze another microscopic discriminator

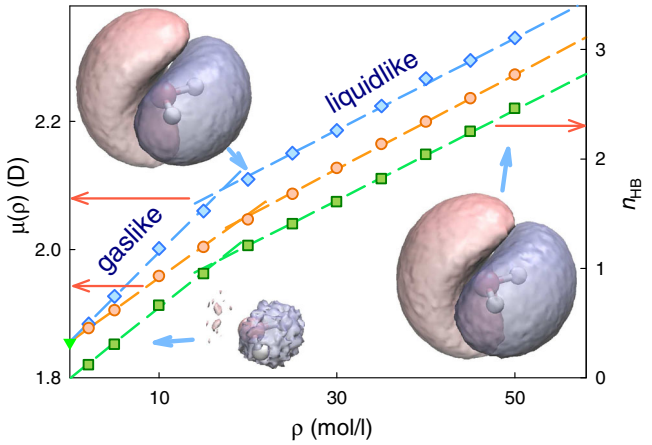

FIG. 1 (color online). Average molecular dipole moment as a function of density at $T = 673$ K (blue diamonds), and at $T =$ 873 K (orange circles). The triangle denotes the isolated monomer value (parameter of the model). Green squares and right scale, average number of hydrogen bonds per molecule as a function of density at $T = 673$ K. The lines are linear fits to the data. Insets illustrate the variation in electron density with pressure, where the pink and blue isosurfaces correspond to gain and loss of electron density.

between the liquidlike and gaslike states: hydrogen bonding. Although the presence of a HB network in the supercritical region is well established by various techniques [22–24], its structure and topology in liquid water is a matter of discussion [24–27]. Examining HB connectivity, we find that local tetrahedral order persists down to low gaslike densities at supercritical temperatures. Using the distance-angle geometric definition of the hydrogen bond of Ref. [28], we observe a similar, albeit less pronounced, crossover in density dependence of the average number of hydrogen bonds per molecule, which occurs at the same densities as the crossover in dipole moment, shown in Fig. 1.

The number of hydrogen bonds per molecule at 673 K and density $\rho = 30$ mol/l (0.54 g/cm^3) is 40% of that of ambient water, 300 K, 55.32 mol/l, where $n_{HB} = 3.71$. This can be compared with 29% of ambient water at the same temperature and 28.9 mol/l estimated from NMR chemical shift measurements [22]. The number of hydrogen bonds per molecule at the crossover density, which decreases slightly from 1.08 at $T = 673$ K to 0.85 at $T = 1083$ K, is well below the percolation threshold, which occurs at $n_{HB} = 1.53(5)$ according to Ref. [29]. This observation is in accord with Raman scattering experiments [27], which are interpreted to indicate no tetrahedral hydrogen bonding at the critical point. We note that collective properties that may show dynamic or viscoelastic anomalies may also be detectable by x-ray scattering techniques or other experimental probes of relaxation processes. We therefore conclude that the onset of the formation of minimal HB associations corresponds to the dipole crossover point in the supercritical field which,

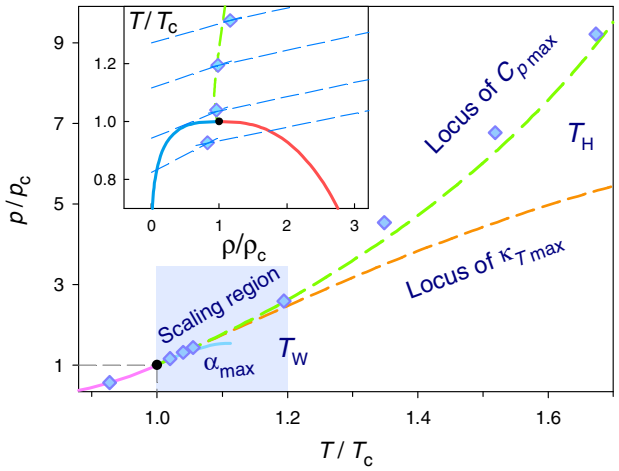

FIG. 2 (color online). (T, p) phase diagram of water in the proximity of the critical point in units of critical temperature T_c and critical pressure p_c. The liquid-vapor coexistence curve (pink), the loci of maxima in heat capacity (green), thermal expansivity (orange), and isothermal compressibility (blue), obtained using the IAPWS-95 reference equation of state [20]. The blue diamonds represent our results derived from the analysis of Fig. 1. The black dot marks the critical point. The inset, the corresponding (ρ, T) phase diagram in reduced units, shows the gas and liquid branches of the coexistence curve, the locus of the heat capacity maxima, and superimposed are linear fits to the dipole moment (the blue dashed lines) in gaslike and liquidlike regions with vertical offsets to map the corresponding temperatures at the crossover. The crossover densities are denoted by the diamonds.

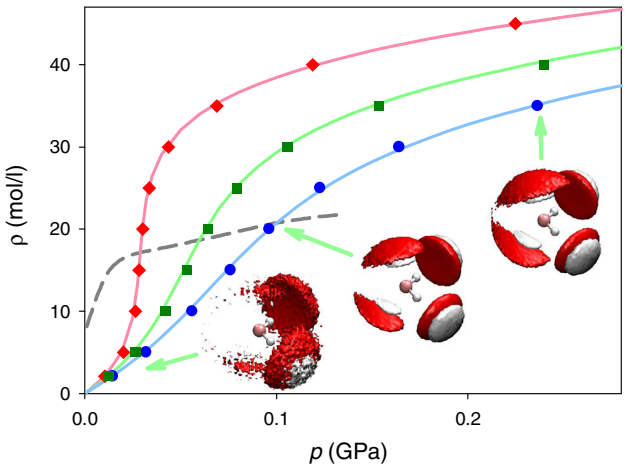

FIG. 3 (color online). Density of water along the $T = 673$, 773, and 873 K isotherms (from top to bottom) as obtained in APIMD QDO simulation (symbols) versus experimental data (full lines). All simulated states, apart from the first four in each isotherm, are in the supercritical region [2]. The dashed line indicates the crossover densities. 3D plots (insets) showing first oxygen (red) and hydrogen (white) coordination shells, illustrate remarkable persistence of tetrahedral structure at $T = 673$ K.

with decreasing temperatures, evolves to the liquid-gas coexistence line in the two-phase region.

The results of the study are summarized in Fig. 2, where we plot the positions of the observed crossover points in the (T, p) plane along with the portion of the coexistence line ending in the critical point and experimental data showing maxima in various response functions. Shown here are specific heat C_p, isothermal compressibility κ_T, and thermal expansivity α. Asymptotically close to the critical point, in the region $T_c < T < T_W$, the dipole crossover points occur along the Widom line, where the loci of all response function maxima coincide. Moreover, the dipole values are unambiguously vaporlike on the low-p side and liquidlike on the high-p side. On the molecular scale it therefore appears possible to extend partially the notion of coexistence and the liquid-gas transition well into the thermodynamically single-phase fluid as a remnant.

At higher temperatures, in the nonasymptotic region $T_W < T < T_H$, the loci of response function maxima diverge from the Widom line, but it appears that the dipole crossover most closely tracks $C_p(T)$. Above T_H the dipole derivative transition becomes undetectable and fluid appears homogeneous at all length scales. We note that the formation of HB dimers creates an additional thermal reservoir that contributes to the specific heat in liquid water. We therefore speculate that this may be the molecular origin of the close link revealed here between dipole-crossover, hydrogen-bond formation, remnant liquid-gas coexistence behavior in the supercritical phase and the locus of maxima in C_p in and beyond the scaling region. No such direct link exists between HB formation and thermal expansivity or isothermal compressibility, the maxima of which follow very different trajectories out of the scaling region.

Finally, we examine the structure and density at several thermodynamic state points for which experimental data are available [30]. We focus first on the $T = 673$ K isotherm and compare the results to neutron diffraction measurements [30]. Predicted densities along this isotherm are shown in Fig. 3 together with data obtained from the IAPWS-95 reference equation of state [20]. Since our QDO model does not involve any condensed-phase parametrization, the agreement arises as a prediction and gives confidence in the previously presented results.

Further structural data are presented in the insets of Fig. 3, which show three-dimensional first coordination shell plots for oxygen (red) and hydrogen (white) of surrounding water molecules. The isosurfaces are drawn at 2× (bulk density) levels. These illustrate the extent of hydrogen-bond reconfiguration which occurs at various densities along the isotherm. The partial radial distribution functions are shown in Fig. 4 for $T = 673$ K, $p =$ 340 MPa (red lines) in comparison to the neutron diffraction data of Ref. [30] (blue lines). Subtle features of the experimental H–H distributions are present in the model, and the O–O correlations are captured as well.

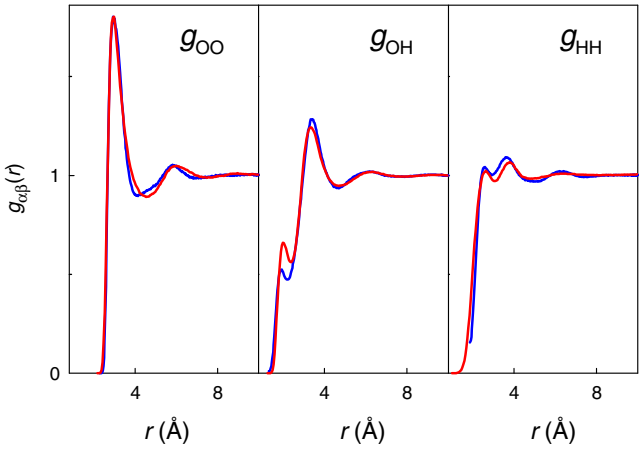

FIG. 4 (color online). The partial radial distribution functions obtained in the QDO water model simulation under supercritical conditions at $T = 673$ K and $p = 340$ MPa (red lines). Also shown for comparison are distribution functions obtained from neutron scattering [30] at the same thermodynamic conditions (blue lines).

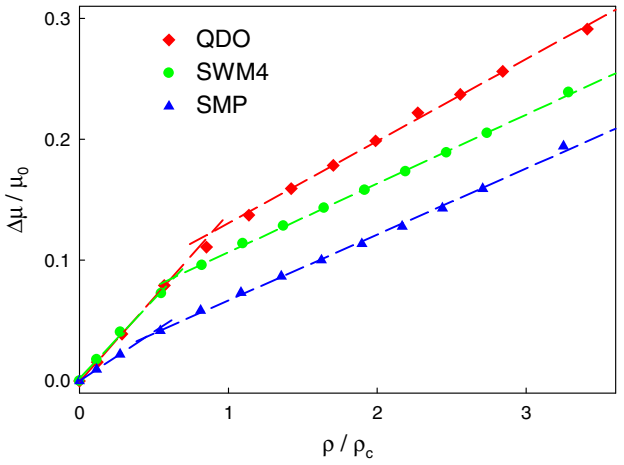

FIG. 5 (color online). Relative (to the gas-phase value) enhancement of the molecular dipole moment as a function of the reduced density. Red diamonds, quantum Drude model; green circles, classical Drude oscillator model (dipole limit); blue triangles, polarizable Stockmayer model (dipole limit). All calculations were performed at a reduced temperature $T^* = 1.036T_c$ in terms of corresponding critical temperature T_c. Straight lines are to guide the eye.

In Fig. 1, the mean molecular dipole moment $|\bar{\mu}|$ is seen to vary linearly with density in two regions, which can be understood using the following argument: The induced dipole moment is proportional to the local field acting on a water molecule, which can be decomposed into contributions from the first coordination shell and from the rest of the fluid. As *ab initio* and induction model calculations of small water clusters [31] have shown, the water dipole moment scales linearly with the cluster size for up to five members in the cluster. A mean-field estimate assuming the average distance to scale like $\rho^{-1/3}$ leads to the same conclusion. More deeply, the Onsager reaction field strength scales linearly with density [32].

For strongly associated liquids like water, the Widom line has been connected with a percolation transition in the hydrogen-bond network [33]. However, our results support the view that the origin of the crossover and the extrema in the response functions is more local. We show that this behavior extends much farther into the notionally one-phase region and can be detected as far as $T = 1.7T_c$, tracking most closely the maxima in the specific heat. Only along the isotherms beyond these temperatures does it appear that supercritical water is a homogeneous fluid on the molecular scale exhibiting no detectable remnants of the liquid-gas transition. The extent of hydrogen bonding across the Widom line and beyond the scaling region can, in principle, be indirectly accessed by Raman scattering measurements of the OH stretch band, which is a reporter of hydrogen bonding and the integrity of the network [27]. Collective properties that may show dynamic or viscoelastic anomalies may also be detectable by x-ray scattering techniques or other experimental probes of relaxation processes.

In order to address the question of generality of the phenomena reported here, we studied two dipole-polarizable models (polarization treated in the electric dipole limit), namely, the classical Drude oscillator model, SWM4-NDP [34], for which the critical parameters are known [35]: $T_c^{\mathrm{dip}} = 0.89T_c$, $p_c^{\mathrm{dip}} = 0.90p_c$, $\rho_c^{\mathrm{dip}} = 1.02\rho_c$, in terms of experimental values for water. The second is a polarizable version of the Stockmayer model, the "minimalist" (purely dipolar) fluid model with a different local association topology [36], and estimated critical parameters $T_c^s = 1.1T_c$, $p_c^s = 1.5p_c$, $\rho_c^s = 1.02\rho_c$ (see Ref. [14]). Finite size effects are investigated and ruled out in Supplemental Material [14]. The results for three models, presented in Fig. 5, show that the dipole moment change is most pronounced in fully responsive QDO, but also emerges from a dipole-polarizable water model and the polarizable Stockmayer model. The reduced crossover density for the QDO model $\rho_\times^* = 0.90$, and shifts to 0.63 for SWM4-NDP and to 0.56 for the Stockmayer model. Therefore, our study has revealed an intriguing new property of associating liquids, the extension of gas-liquid critical effects on the molecular dipole moment.

In summary, we find direct evidence of molecular-scale heterogeneity in supercritical polar fluids. A clearly identifiable transition between dissociated (gaslike) and associated (liquidlike) regimes is evidenced by a change in the density dependence of the molecular dipole moment accompanied by a transition in the hydrogen-bond connectivity. This characteristic signature has been observed in a fully responsive electronic model of water which provides an excellent prediction of the ambient, critical, and supercritical properties but is also present in simpler dipole-limit models with two different association topologies—the minimal model class in which the behavior may be observed. While the simpler models do not predict the

critical point accurately for water, they nevertheless provide compelling evidence that the phenomenon is likely to be general for polar liquids. The observations provide a molecular basis for the variety of response function anomalies that define the "Widom line" asymptotically close to the critical point. This is also significant outside the scaling regime where the maxima of thermodynamic response functions follow different trajectories making it unclear which, if any, separate liquidlike from gaslike regions. Here we observe that the dipole crossover points follow only the heat capacity maximum outside of the scaling region and their correlation to rudimentary hydrogen bonding establishes an unambiguous extension of the liquid-gas coexistence line deep into the supercritical phase.

This work was supported by the NPL Strategic Research program, the Engineering and Physical Sciences Research Council (EPSRC), and the European Metrology Research Programme (EMRP). Generous allocation of time on BG/Q at STFC Hartee Centre, UK, is gratefully acknowledged.

[1] H. E. Stanley, *Introduction to Phase Transitions and Critical Phenomena* (Oxford University Press, New York, 1971).
[2] *Supercritical Fluids*, edited by Y. Arai, T. Sako, and Y. Takebayashi (Springer, Berlin, 2002).
[3] N. Akiya and P. E. Savage, Chem. Rev. **102**, 2725 (2002).
[4] C. A. Eckert, B. L. Knutson, and P. G. Debenedetti, Nature (London) **383**, 313 (1996).
[5] V. V. Brazhkin, Y. D. Fomin, A. G. Lyapin, V. N. Ryzhov, and E. N. Tsiok, J. Phys. Chem. B **115**, 14112 (2011).
[6] L. Xu, P. Kumar, S. V. Buldyrev, S.-H. Chen, P. H. Poole, F. Sciortino, and H. E. Stanley, Proc. Natl. Acad. Sci. U.S.A. **102**, 16558 (2005).
[7] G. G. Simeoni, T. Bryk, F. A. Gorelli, M. Krisch, G. Ruocco, M. Santoro, and T. Scopigno, Nat. Phys. **6**, 503 (2010).
[8] M. J. Gillan, D. Alfè, A. P. Bartók, and G. Csányi, J. Chem. Phys. **139**, 244504 (2013).
[9] V. P. Sokhan, A. Jones, J. Crain, F. Cipcigan, and G. Martyna, Proc. Natl. Acad. Sci. U.S.A. **112**, 6341 (2015).
[10] T. W. Whitfield and G. J. Martyna, Chem. Phys. Lett. **424**, 409 (2006).
[11] T. W. Whitfield and G. J. Martyna, J. Chem. Phys. **126**, 074104 (2007).
[12] A. P. Jones, J. Crain, V. P. Sokhan, T. W. Whitfield, and G. J. Martyna, Phys. Rev. B **87**, 144103 (2013).
[13] A. Jones, F. Cipcigan, V. P. Sokhan, J. Crain, and G. J. Martyna, Phys. Rev. Lett. **110**, 227801 (2013).
[14] See Supplemental Material at http://link.aps.org/supplemental/10.1103/PhysRevLett.115.117801, which includes Refs. [15–19], for the Drude model parameters and simulation details.
[15] A. Jones, A. Thompson, J. Crain, M. H. Muser, and G. J. Martyna, Phys. Rev. B **79**, 144119 (2009).
[16] G. J. Martyna, M. E. Tuckerman, D. J. Tobias, and M. L. Klein, Mol. Phys. **87**, 1117 (1996).
[17] A. Jones, J. Crain, F. Cipcigan, V. Sokhan, M. Modani, and G. Martyna, Mol. Phys. **111**, 3465 (2013).
[18] A. Jones and B. Leimkuhler, J. Chem. Phys. **135**, 084125 (2011).
[19] J. C. Phillips, R. Braun, W. Wang, J. Gumbart, E. Tajkhorshid, E. Villa, C. Chipot, R. D. Skeel, L. Kal, and K. Schulten, J. Comput. Chem. **26**, 1781 (2005).
[20] W. Wagner and A. Pruß, J. Phys. Chem. Ref. Data **31**, 387 (2002).
[21] J. D. Bernal and R. H. Fowler, J. Chem. Phys. **1**, 515 (1933).
[22] M. M. Hoffmann and M. S. Conradi, J. Am. Chem. Soc. **119**, 3811 (1997).
[23] P. Wernet, D. Testemale, J.-L. Hazemann, R. Argoud, P. Glatzel, L. G. M. Pettersson, A. Nilsson, and U. Bergmann, J. Chem. Phys. **123**, 154503 (2005).
[24] M. Bernabei, A. Botti, F. Bruni, M. A. Ricci, and A. K. Soper, Phys. Rev. E **78**, 021505 (2008).
[25] P. Wernet, D. Nordlund, U. Bergmann, M. Cavalleri, M. Odelius, H. Ogasawara, L. Å. Näslund, T. K. Hirsch, L. Ojamäe, P. Glatzel, L. G. M. Pettersson, and A. Nilsson, Science **304**, 995 (2004).
[26] T. Head-Gordon and M. E. Johnson, Proc. Natl. Acad. Sci. U.S.A. **103**, 7973 (2006).
[27] Q. Sun, Q. Wang, and D. Ding, J. Phys. Chem. B **118**, 11253 (2014).
[28] R. Kumar, J. R. Schmidt, and J. L. Skinner, J. Chem. Phys. **126**, 204107 (2007).
[29] R. L. Blumberg, H. E. Stanley, A. Geiger, and P. Mausbach, J. Chem. Phys. **80**, 5230 (1984).
[30] A. K. Soper, Chem. Phys. **258**, 121 (2000).
[31] J. K. Gregory, D. C. Clary, K. Liu, M. G. Brown, and R. J. Saykally, Science **275**, 814 (1997).
[32] L. Onsager, J. Am. Chem. Soc. **58**, 1486 (1936).
[33] L. B. Pártay, P. Jedlovszky, I. Brovchenko, and A. Oleinikova, J. Phys. Chem. B **111**, 7603 (2007).
[34] G. Lamoureux, E. Harder, I. V. Vorobyov, B. Roux, and A. D. MacKerell, Jr., Chem. Phys. Lett. **418**, 245 (2006).
[35] P. T. Kiss and A. Baranyai, J. Chem. Phys. **137**, 194103 (2012).
[36] M. van Leeuwen, Fluid Phase Equilib. **99**, 1 (1994).